Green Chemistry

PAPER

View Article Online
View Journal | View Issue

Cite this: *Green Chem.*, 2025, **27**, 642

Constructing a chemoenzymatic strategy for enhancing the efficiency of selectively transforming 5-hydroxymethylfurfural into furan carboxylic acids†

Zhiyu Zhang,‡[a] Xiaowang Zhang,‡[a] Siyu Qi,[a] Qi Na,[a] Kaichen Zhao,[a] Ziyi Yu,[b] Zhuotao Tan,*[a] Hanjie Ying [a] and Chenjie Zhu *[a]

Furan carboxylic acids including 5-hydroxymethyl-2-furancarboxylic acid (HMFCA), 5-formyl-2-furancarboxylic acid (FFCA) and 2,5-furandicarboxylic acid (FDCA) are important bio-based chemicals and widely applied in the fields of pharmaceuticals and materials. However, selectively obtaining these value-added compounds from biomass-derived 5-hydroxymethylfurfural (HMF) is difficult due to the readily reactive alcohol/aldehyde groups of the generated intermediates during the oxidative process. Biotransformation using enzyme catalysis is a sustainable and promising approach, but there are remaining challenges including low efficiency and selectivity due to the chaotic and complex biocatalytic process, loss of enzyme activity and inevitable increase in reaction volume caused by exogenous addition of H_2O_2. In these contexts, a natural flavin cofactor mimic (NFCM)-mediated chemoenzymatic system consisting of H_2O_2-dependent peroxygenase, NAD^+-dependent alcohol dehydrogenase and galactose oxidase was constructed for the first time for selectively converting HMF to each furan carboxylic acid. The bifunctional catalyst NFCM enabled the *in situ* generation of H_2O_2 and regeneration of NAD^+, which skillfully alleviated the problems caused by exogenous addition of H_2O_2. Each furan carboxylic acid was achieved with excellent yield (>99%) and selectivity (>99%). Furthermore, an immobilization technique based on a hydrogel material was employed for the first time, which greatly promoted the stability and reusability of each biocatalyst.

Received 21st September 2024,
Accepted 5th December 2024

DOI: 10.1039/d4gc04735d

rsc.li/greenchem

Green Foundation

1. This work demonstrated a green and efficient chemoenzymatic cascade system, which could selectively transform HMF into each value-added furan carboxylic acid.
2. The whole reaction system was carried out in the aqueous phase, and no by-product was accumulated, which facilitated the subsequent separation and purification of products. Furthermore, the *E*-factor and atom efficiency of this system were calculated, which showed apparent advantages among the reported systems.
3. Further work about enhancing the enzyme tolerance to the substrate concentration through dehydrogenase evolution, which could increase the space–time yields of each furan carboxylic acid, is underway in our lab.

1. Introduction

With the growth in the demand and diminishing of the reserves of fossil fuels, it is urgent to develop sustainable sources for fuels and chemicals.[1] Lignocellulosic biomass is the most attractive alternative due to its abundance, low cost, and sustainable properties.[2] 5-Hydroxymethylfurfural (HMF) is one of the top-value platform chemicals derived from biomass.[3,4] Based on the active alcohol hydroxyl and aldehyde groups, HMF can be easily oxidized into other value-added

[a]*College of Biotechnology and Pharmaceutical Engineering, Nanjing Tech University, 30 S Puzhu Rd, 211816 Nanjing, China. E-mail: joh_yy@njtech.edu.cn, zhucj@njtech.edu.cn*
[b]*State Key Laboratory of Materials-Oriented Chemical Engineering, College of Chemical Engineering, Nanjing Tech University, 30 S Puzhu Rd, 211816 Nanjing, China*

†Electronic supplementary information (ESI) available. See DOI: https://doi.org/10.1039/d4gc04735d

‡These authors contributed equally to this paper.

furan carboxylic acids which have great application potential in fuels, fine chemicals, polymers, medical intermediates, *etc*.[5] For example, 5-hydroxymethyl-2-furancarboxylic acid (HMFCA) is an important precursor of pharmaceutical intermediates.[6,7] 5-Formyl-2-furancarboxylic acid (FFCA) and 2,5-furandicarboxylic acid (FDCA) are promising building blocks for the manufacture of polymers.[8,9] Generally, the conversion of HMF to these valuable furan carboxylic acids can be divided into two different oxidation pathways: the aldehyde oxidation pathway (route 1) and the alcohol oxidation pathway (route 2) (Scheme 1A). However, due to the readily oxidizing reactive aldehyde/alcohol groups of each compound during the oxidation process, it is difficult to selectively transform HMF into each furan carboxylic acid. Although various valuable chemical methods have been reported for oxidizing HMF, these approaches rely on metals and are carried out under harsh conditions with low selectivity.[10–13] Recently, biological oxidation of HMF has emerged as a favorable and promising alternative due to its mild reaction conditions and environmental friendliness.[14,15] Several isolated enzyme catalysis approaches using O_2-dependent oxidases, H_2O_2-dependent peroxygenases, and NAD(P)$^+$-dependent dehydrogenases for the oxidation of HMF have been reported.[16–19] However, these enzymes usually tend to competitively catalyze the aldehyde/alcohol substrate (intermediate) during the bio-oxidation of HMF.[20–23] The resulting chaotic and complex biocatalytic process restricts the selectivity and efficiency of bio-oxidation of HMF to each furan carboxylic acid.[20–22] Thus, constructing a simple, orderly, and efficient system that can selectively transform HMF into each furan carboxylic acid is highly desirable.

Moreover, H_2O_2 has been employed as an oxidative alternative to O_2 in the biotransformation of HMF, which can alleviate the challenge of oxygen dissolution and mass transfer problem.[22,23] However, the enzymes used in the bio-oxidation of HMF are often H_2O_2 concentration sensitive.[22] Exogenous addition of excess amount of H_2O_2 not only leads to irreversible enzyme deactivation but also inevitably results in the increase of the reaction volume,[24–26] which impairs the reaction efficiency. Recently, an *in situ* H_2O_2 generation and utilization multi-enzyme catalytic system including dehydrogenase, horseradish peroxidase (HRP), and oxidase was developed to selectively bio-oxidize HMF to furan carboxylic acid (Scheme 1A).[23] However, there are still some drawbacks as follows: (1) for the synthesis of HMFCA, exogenous addition of H_2O_2 was still required; (2) the expensive electron transporter scopoletin[27] was required to enable NAD$^+$ regeneration for dehydrogenase during the catalytic process, which generated free radicals and resulted in the loss of enzyme activity; and (3) low turnover numbers (TONs). In these contexts, it is highly attractive to develop a novel and effective *in situ* H_2O_2 generation and utilization system that does not impair the enzyme activity to promote the selective biotransformation of HMF into each furan carboxylic acid.

Recently, H_2O_2-dependent unspecific peroxygenase (UPO) has been demonstrated as an efficient and robust biocatalyst for HMF biotransformation, but the exogenous addition of H_2O_2 is still required to drive the reaction and the chemoselectivity of UPO was unsatisfactory. Our previous studies have shown that NFCM can oxidize reduced nicotinamide coenzyme NADH to regenerate NAD$^+$ for the ADH-catalyzed oxidation reaction, which could produce H_2O_2 with the consumption of molecular oxygen.[28,29] We wonder if UPO could be coupled with a HLADH–NFCM system, thereby constructing a novel chemoenzymatic system to boost the selective biotransformation of HMF. During the catalytic process, UPO-catalyzed oxidation of HMF or FFCA was enhanced by coupling with NAD$^+$-dependent alcohol dehydrogenase from horse (HLADH). NFCM was responsible for regenerating NAD$^+$ and *in situ* generating H_2O_2, which are required for ADH and UPO catalysis, respectively (Scheme 1B). Furthermore, galactose oxidase (GOase) was employed to selectively oxidize HMFCA to FFCA (Scheme 1B).[23] Herein, employing UPO, HLADH, and GOase, we proposed a novel one-pot NFCM-mediated chemoenzymatic system that could selectively convert HMF to each value-added furan carboxylic acid with high efficiency (Scheme 1B). The immobilization strategy was further explored to enable the recycling of the biocatalysts, facilitating the further scale-up of HMF derivative production.

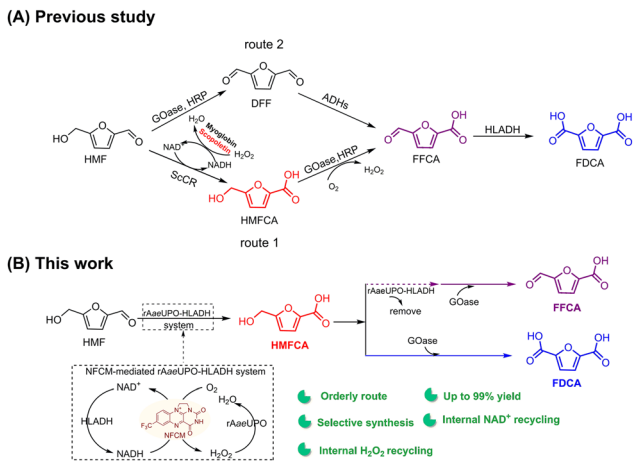

Scheme 1 The previous and current strategies for the selective synthesis of HMFCA, FFCA and FDCA. (A) Previous study. (B) This work.

2. Results and discussion

2.1 The selective synthesis of HMFCA from HMF

Firstly, we investigated the possibility of UPO-catalyzed selective conversion of HMF to HMFCA. The recombinant evolved unspecific peroxygenase derived from *Agrocybe aegerita* (rA*ae*UPO) was chosen for the oxidation reactions.[30] In the initial experiments, one equivalent amount of H_2O_2 was added continuously to drive the rA*ae*UPO-catalyzed oxidation of HMF. As shown in Table 1 (entry 1), a yield of only 29% HMFCA was obtained. The by-products DFF, FFCA, and FDCA were also observed with yields of 16%, 8%, and 1%, respectively. In

Table 1 The oxidation of HMF to HMFCA catalyzed by rAaeUPO

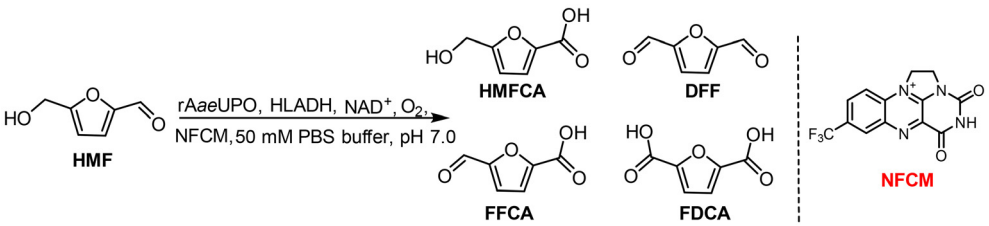

						Yield [%]			
Entry	rA*ae*UPO [μM]	HLADH [μM]	NFCM [mM]	H_2O_2 [mM]	Conversion [%]	HMFCA	DFF	FFCA	FDCA
1[a]	1	—	—	10	54	29	16	8	1
2[b]	1	—	0.02	—	80	43	23	13	1
3[c]	—	2	0.02	—	16	14	1	1	—
4[d]	1	2	0.02	—	90	88	—	—	2
5[e]	0.1	0.08	0.02	—	100	>99	—	—	—

[a] Reaction conditions: 10 mM HMF and 1 μM rA*ae*UPO were added into 1 mL of phosphate buffer (50 mM, pH 7.0), and 10 mM H_2O_2 was added continuously over 12 h. [b] Reaction conditions: 10 mM HMF, 1 μM rA*ae*UPO, and 10 mM NADH were added into 1 mL of phosphate buffer (50 mM, pH 7.0). [c] Reaction conditions: 10 mM HMF, 2 μM HLADH, 0.02 mM NFCM, and 0.1 mM NAD^+ were added into 1 mL of phosphate buffer (50 mM, pH 7.0). [d] Reaction conditions: 10 mM HMF, 1 μM rA*ae*UPO, 2 μM HLADH, 0.02 mM NFCM, and 0.1 mM NAD^+ were added into 1 mL of phosphate buffer (50 mM, pH 7.0). [e] Reaction conditions: 10 mM HMF, 0.1 μM rA*ae*UPO, 0.08 μM HLADH, 0.02 mM NFCM, and 0.1 mM NAD^+ were added into 1 mL of phosphate buffer (50 mM, pH 7.0). The concentration of each product was quantified by HPLC, which was equipped with an Aminex HPX-87H column (300 mm × 7.8 μm), and the methods are listed in section 1.8 of the ESI.†

addition, the continuous addition of H_2O_2 led to a 10% increase in the reaction volume and a 30% decrease in the catalytic activity of rA*ae*UPO (Fig. S1†).[22] To alleviate this dilemma, our reported *in situ* H_2O_2 generation system using NFCM as the catalyst and NAD(P)H as a hydrogen donor was employed to couple with rA*ae*UPO for the transformation of HMF.[29] The result showed that the conversion and yield of the desired product HMFCA were both increased when compared to that with the continuous addition of H_2O_2 (Table 1, entry 2), but the chemoselectivity of rA*ae*UPO remained unsatisfactory. We attributed this to the chaotic oxidative reactivity of rA*ae*UPO towards alcohol/aldehyde groups. Hence, we speculated that the selectivity and efficiency of this reaction could be enhanced by coupling with NAD^+-dependent HLADH, which also can oxidize HMF. Moreover, further considering the high cost of the chemical equivalent NAD(P)H, we also intended to employ HLADH to regenerate this hydrogen donor in the case of HMF oxidation.[27] Thus, a NFCM-mediated rA*ae*UPO–HLADH chemoenzymatic system was proposed to catalyze HMF to HMFCA (Table 1, entry 3). It could be found that the selectivity of this chemoenzymatic system (Fig. 1A, purple line) was significantly enhanced compared with that of the single UPO-catalyzed biotransformation of HMF (Fig. 1A, red line). 90% of HMF was effectively transformed in 12 h (Fig. 1B), and the yield of HMFCA increased to 88%, with only 2% FDCA obtained as a by-product (Table 1, entry 3). We attributed this significant improvement to the effective recycling of H_2O_2 that alleviated the inhibition of the enzymes and promoted the catalytic efficiency of this reaction.

Considering the remaining unconverted HMF and by-product FDCA, further experiments were conducted to promote the efficiency of the reaction. Initially, we hypothesized that different pH values could affect the dual-enzymatic system, and a significant decrease of the conversion and selectivity was observed under acidic or alkaline conditions compared with that under pH 7.0 (Fig. S2†). Then, we surmised that the kinetic balance of the HLADH and rA*ae*UPO-catalyzed oxidation of HMF was a key factor that affected the reaction efficiency. Hence, we explored if adjusting the quantity of these two enzymes could promote the efficiency of the reaction. As shown in Fig. S3,† increasing the amount of rA*ae*UPO did not have any impact on the reaction. However, the conversion of HMF gradually decreased with the gradually reduced dosage of rA*ae*UPO, while the yield of HMFCA was maintained at a high level (98%). This may be because the enzyme activity was impaired by the generated H_2O_2 that was not consumed by rA*ae*UPO in time. Based on this result, the impact of the HLADH concentration on the reaction efficiency was further explored. As shown in Fig. S4,† the conversion and selectivity decreased sharply when increasing the dosage of HLADH from 2 to 4 μM. This could also be attributed to the over-generated H_2O_2, which in turn affected the enzyme activity. In addition, adding a large amount of enzyme can not only increase the reaction cost but also result in low turnover numbers (TONs), which are obviously infeasible. Surprisingly, on reducing the dosage of HLADH from 2 to 0.08 μM, a remarkable enhancement of conversion (100% *vs.* 90%) and selectivity (>99% *vs.* 98%) was obtained. We can conclude that the kinetics of HLADH and rA*ae*UPO were well balanced under these conditions. Notably, the TON of the enzymes (HLADH and rA*ae*UPO) reached 55 000, which was nearly 10 times higher than that in the reported literature (Table S3†). Other

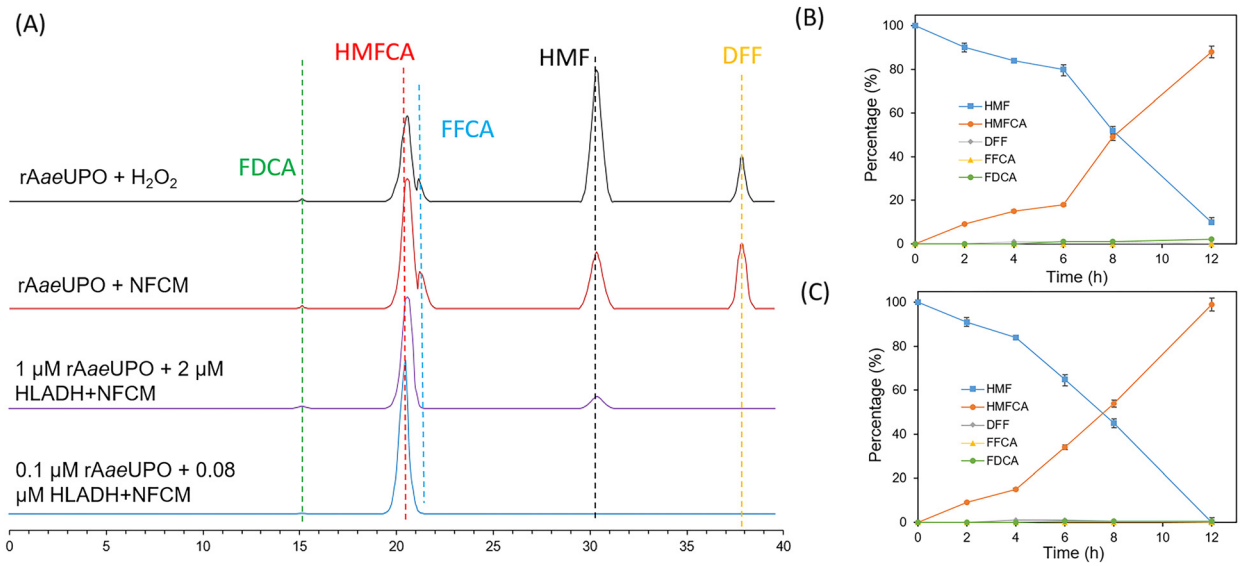

Fig. 1 The chemoenzymatic selective synthesis of HMFCA from HMF. (A) The final state of the chemoenzymatic reaction under different conditions. (B) Time course for the synthesis of HFMCA catalyzed by the initial rA*ae*UPO–HLADH system. (C) Time course for the synthesis of HFMCA under optimal conditions. Reaction conditions: 0.1 mM NAD^+, 0.02 mM NFCM, 10 mM HMF, 0.08 μM HLADH and 0.1 μM rA*ae*UPO were added into 1 mL of phosphate buffer (50 mM, pH 7.0) in turn and shaken at 30 °C. Percentage (%) is the ratio of the concentration of each component and calculated according to the formula given in section 1.8 in the ESI†. The detection methods of each compound were the same as those in Table 1.

metrics of our system including space–time yield, *E*-factor and atom efficiency were also calculated and compared with the reported systems (Table S3†). In the aspects of atom efficiency and *E*-factor, our system is the best among the reported methods.

2.2 The chemoenzymatic selective synthesis of FFCA from HMF by a sequential and stepwise process

Based on the above positive results, the selective conversion of HMF to FFCA was investigated. GOase that could transform HMFCA into FFCA[23] was further employed to couple with the NFCM-mediated rA*ae*UPO–HLADH system for selectively oxidizing HMF to FFCA (Fig. 2A). Firstly, a one-pot concurrent approach that simultaneously added GOase and the NFCM-mediated rA*ae*UPO–HLADH system was proposed. As shown in Fig. 2B, HMF was completely transformed in the first 12 h, but the reaction barely proceeded in the following 12 h with only 47% FFCA detected at the end of the reaction. A large amount of by-product DFF (52%) was detected, which was because GOase could also rapidly convert HMF to DFF.[23] Next, a sequential and stepwise process was proposed to enhance the selectivity of the reaction (Fig. 2A). The NFCM-mediated rA*ae*UPO–HLADH system was firstly added for the transformation of HMF into HMFCA (step 1), and then deactivated by high temperature. Next, GOase was added to the reaction for the following catalysis of HMFCA to FFCA. As expected, HMF was completely transformed in the first 16 h, and then the generated HMFCA was fully oxidized to FFCA by GOase within an additional 8 h (Fig. 2C). The selectivity and yield of the sequential approach were significantly enhanced compared with those of the concurrent approach (99% *vs.* 46%). Notably, the TON of the enzymes reached 8250, which is higher than that of the previous reported system (Table S4†). The atom efficiency and *E*-factor of our system are at moderate levels compared to the previously reported system (Table S4†).

2.3 The chemoenzymatic selective synthesis of FDCA from HMF by a one-pot two-step method

Since the results in Table 1 indicated that rA*ae*UPO was also a promising biocatalyst for the oxidation of FFCA to FDCA, we investigated if NFCM-mediated rA*ae*UPO–HLADH could also be employed for the selective transformation of HMF into FDCA. The initial experiment was conducted to explore the possibility of using the NFCM-mediated rA*ae*UPO–HLADH system to catalyze the transformation of FFCA into FDCA. As shown in Fig. 3B, the yield of FDCA was gradually increased to >99% on adding an *in situ* H_2O_2 generation system (NADH and NFCM) and the NAD^+ recycling system (ADH, NFCM, and NAD^+). This result was similar to that of the above selective transformation of HMF into HMFCA (Table 1). Based on the favorable results, a one-pot, two-step sequential approach using the NFCM-mediated rAaeUPO–HLADH system and GOase for the chemoenzymatic transformation of HMF into FDCA was proposed (Fig. 3A). Notably, unlike the reaction for synthesizing FFCA, HLADH and rA*ae*UPO should not be inactivated (step 2). The results indicated that HMF could be completely converted in 28 h with excellent selectivity and yield of FDCA (>99%) (Fig. 3C). Moreover, we found that no additional HLADH and rA*ae*UPO were required during the reaction. After calculation, the TON of the enzymes in the overall catalytic process was about 8250, which was approximately ~3-fold higher than the reported highest value (Table S5†). Moreover,

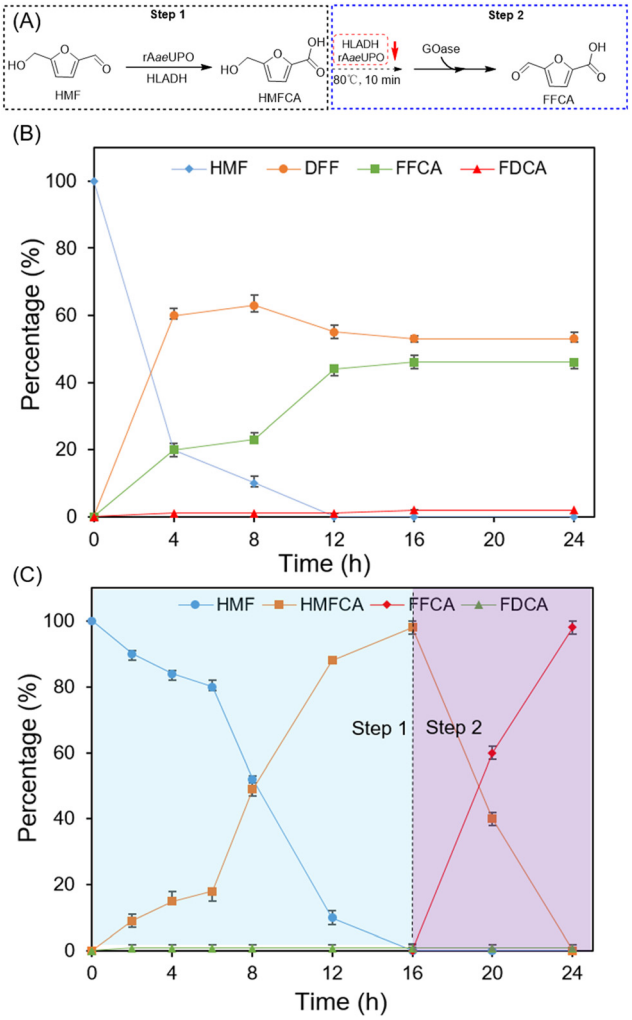

Fig. 2 The chemoenzymatic cascade system for selectively catalyzing the oxidation of HMF to FFCA. (A and C) One-pot two-step method. Reaction conditions: 0.1 mM NAD^+, 0.02 mM NFCM, 10 mM HMF, 0.08 μM HLADH, 0.1 μM rA*ae*UPO and 1 μM GOase were added into 1 mL of phosphate buffer (50 mM, pH 7.0) in turn and shaken at 30 °C (300 rpm). (B) One-pot one-step method. The detection methods of each compound were the same as those in Table 1. Percentage (%) is the ratio of the concentration of each component in the mixture and calculated according to the formula given in section 1.8 in the ESI.†

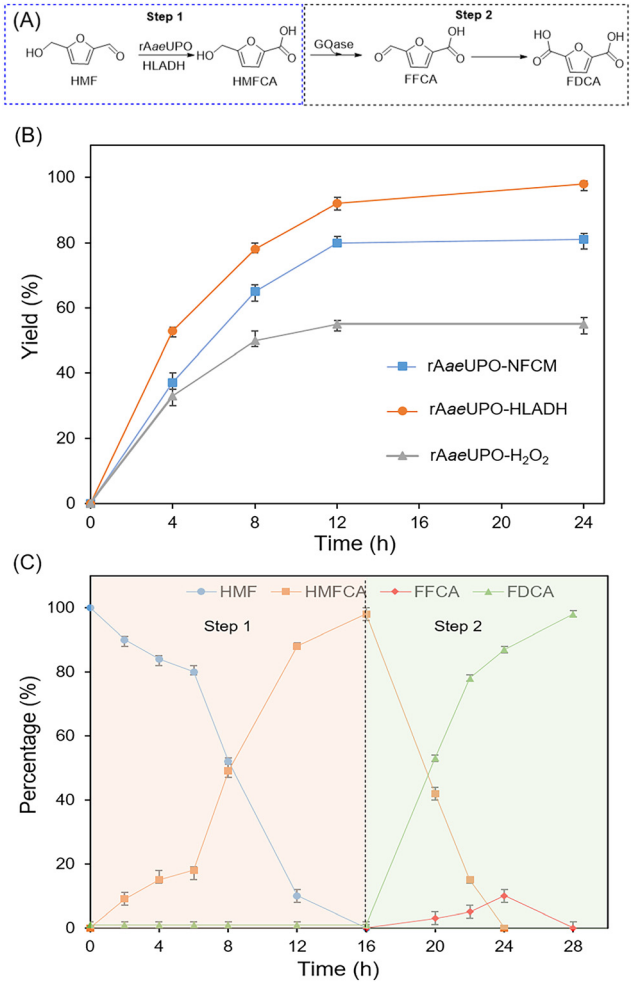

Fig. 3 The selective synthesis of FDCA from HMF. (A and C) One-pot two-step method. Reaction conditions: 0.1 mM NAD^+, 0.02 mM NFCM, 10 mM HMF, 0.08 μM HLADH, 0.1 μM rA*ae*UPO and 1 μM GOase were added into 1 mL of phosphate buffer (50 mM, pH 7.0) in turn and shaken at 30 °C (300 rpm). (B) The oxidation of FFCA to FDCA catalyzed by different chemoenzymatic systems. Reaction conditions and detection methods were the same as those in Table 1. Percentage (%) is the ratio of the concentration of each component in the mixture and calculated according to the formula given in section 1.8 in the ESI.†

our constructed chemoenzymatic system also showed apparent advantages in the aspects of *E*-factor and atom efficiency over other systems (Table S5†).

2.4 The selective synthesis of furan carboxylic acids from HMF catalyzed by immobilized enzymes

Subsequently, we attempted to explore an efficient immobilization method to increase the stability and recyclability of enzymes. Various valuable immobilization strategies including embedding, adsorption, crosslinking and covalent bonding have been proposed.[31,32] Hydrogels, as one of the representative materials employed in covalent binding immobilization technology, have been widely used in the medical field due to their excellent biocompatibility, easy availability, safety, and biodegradability.[33] Recently, we have investigated a novel sodium alginate hydrogel and applied it to cell immobilization and 3D printing.[34] Thus, we wonder if this material could be applied for the immobilization of the above enzymes. As shown in Table 2 (entries 1, 2 and 4) and Fig. S6,† HLADH, rA*ae*UPO, and GOase can be separately and effectively immobilized to a hydrogel material with a high efficiency ranging from 60% to 78%. Moreover, HLADH and rA*ae*UPO could also be co-immobilized to this material with an efficiency of 65% (**E3**). Validation experiments have also shown that immobilized enzymes rarely detach from the hydrogel (Fig. S8†). After confirming the feasibility of the immobilization approach, we first used the co-immobilized **E3** for catalyzing HMF to HMFCA. As

Table 2 The comparison of efficiency before and after enzyme immobilization

Entry	Sample	Activity[a] [U mg^{-1}]	Activity[b] [U mg^{-1}]	Immobilization efficiency[c] [%]
1	**E1** (HLADH)	0.1	0.042	70
2	**E2** (rA*ae*UPO)	257	121	60
3	**E3** (HLADH and rA*ae*UPO)	0.1 257	0.037 118	65
4	**E4** (GOase)	75	30	78

[a] Activity of free enzymes. [b] Activity of co-immobilized enzymes or immobilized enzymes. [c] The immobilization efficiency was calculated according to the formula given in section 1.7 in the ESI†.

shown in Fig. 4A, complete conversion was observed at 10 mM HMF in 24 h, proving the viability of the co-immobilization approach. Next, we determined the recyclability of the co-immobilized enzymes. The results in Fig. 4B show that **E3** could be reused at least 7 times, while maintaining an above 80% yield. These results clearly demonstrated a significant enhancement in the stability of immobilized enzymes compared with that of free enzymes. Subsequently, we further verified the feasibility of coupling **E3** with **E4** for the selective transformation of HMF into FFCA. As expected, the reaction proceeded smoothly in the first cycle, yielding 98% FFCA in 32 h (Fig. 4C). Notably, the operation of heat deactivation of the free enzyme-catalysis (Fig. 2) was replaced by the simple operation of taking out of the immobilized **E3**, which enabled the reuse of **E3**. With this modified procedure, **E3** and **E4** could be recycled 6 times. The yield of FFCA of each cycle was maintained above 98% (Fig. 4D). Then, the immobilized enzymes **E3** and **E4** were applied to catalyze the selective oxidation of HMF to FDCA by a one-pot two-step sequential approach. As shown in Fig. 4E, 99% yield of FDCA was obtained after 28 h. Based on the results, we explored the recyclability of **E3** and **E4** for converting HMF to FDCA. As expected, the system could also be recycled up to 6 times without any decrease in the yield (98%) (Fig. 4F). Finally, for isolating the product, we changed the analytical scale conditions to a semi-preparative scale (1.26 g). Under these conditions, HMFCA, FFCA, and FDCA were all obtained with excellent analytical yield (>98%) and selectivity (>99%), respectively (Table S6†). Each product was obtained in pure form with 79%–85% isolated yield (Table S6†).

3. Conclusions

In summary, we have developed an orderly and efficient NFCM-mediated chemoenzymatic cascade system, which could selectively transform HMF into each value-added furan carboxylic acid. The organocatalyst NFCM acts as a bifunctional catalyst, which enables *in situ* generation of H_2O_2 and regeneration of NAD^+ for ADH and UPO-catalyzed oxidation of HMF, thereby promoting efficiency and selectivity of each oxidation reaction. HMFCA, FFCA, and FDCA were all obtained with excellent yield (>99%) and selectivity (>99%).

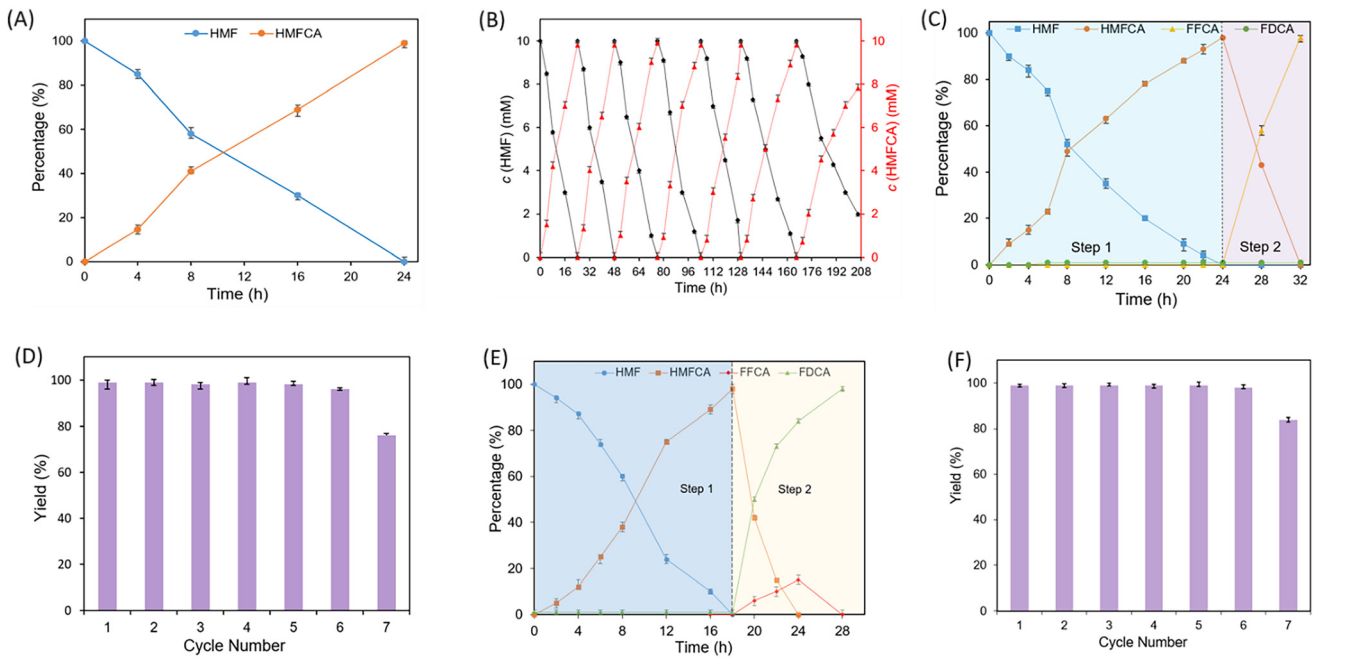

Fig. 4 The immobilized enzymes selectively oxidized HMF to produce HMFCA, FFCA and FDCA. (A and B) For HMFCA. Reaction conditions: 0.1 mM NAD^+, 0.02 mM NFCM, 10 mM HMF, 0.08 or 0.16 μM HLADH and 0.1 or 0.2 μM rA*ae*UPO were added into 2 mL of phosphate buffer (50 mM, pH 7.0) in turn. (C and D) For FFCA. After HMF was completely transformed, HLADH and rA*ae*UPO were taken out and 2 μM GOase was added, and the mixture was shaken at 30 °C (300 rpm). (E and F) For FDCA. Reaction conditions: 0.24 μM HLADH and 0.3 μM rA*ae*UPO were used. Percentage (%) is the ratio of the concentration of each component in the mixture and calculated according to the formula given in section 1.8 in the ESI.†

Furthermore, the stability and reusability of each biocatalyst were greatly improved by a sodium alginate hydrogel-based immobilizing strategy. This first example of chemoenzymatic strategy not only offers a promising approach for the selective synthesis of furan carboxylic acids from HMF, but also presents a flexible and mutually beneficial approach that couple-sperоxygenase with dehydrogenase for enhancing the efficiency of other selective biocatalytic oxidations. Further work on expanding the application scope of this remarkable system is under investigation in our lab.

Author contributions

Xiaowang Zhang: investigation and writing of the original draft. Zhiyu Zhang: investigation and writing of the original draft. Zhuotao Tan and Ziyi Yu: methodology and resources. Siyu Qi: methodology and investigation. Qi Na: supervision and data curation. Kaichen Zhao: methodology and validation. Hanjie Ying: methodology, supervision, and validation. Chenjie Zhu: supervision, conceptualization, reviewing, and editing.

Data availability

The data supporting this article have been included as part of the ESI.†

Conflicts of interest

There are no conflicts to declare.

Acknowledgements

This work was supported by the National Key R&D Program of China (grant no. 2022YFC2105900) and the National Natural Science Foundation of China (grant no. 22378195; 22178170; 22208156).

References

1 J. J. Bozell and G. R. Petersen, *Green Chem.*, 2010, **12**, 539–554.
2 R. A. Sheldon, *Curr. Opin. Green Sustainable Chem.*, 2018, **14**, 89–95.
3 X. Wu, M. V. Galkin, T. Stern, Z. Sun and K. Barta, *Nat. Commun.*, 2022, **13**, 3376–3387.
4 R. Rinaldi, R. Jastrzebski, M. T. Clough, J. Ralph, M. Kennema, P. C. A. Bruijnincx and B. M. Weckhuysen, *Angew. Chem., Int. Ed.*, 2016, **55**, 8164–8215.
5 K. Gu, D. Wang, C. Xie, T. Wang, G. Huang, Y. Liu, Y. Zou, L. Tao and S. Wang, *Angew. Chem., Int. Ed.*, 2021, **60**, 20253–20258.
6 J. J. Pacheco and M. E. Davis, *Proc. Natl. Acad. Sci. U. S. A.*, 2014, **111**, 8363–8367; A. C. Braisted, J. D. Oslob, W. L. Delano, J. Hyde, R. S. McDowell, N. Waal, C. Yu, M. R. Arkin and B. C. Raimundo, *J. Am. Chem. Soc.*, 2003, **125**, 3714–3715.
7 K. T. Hopkins, W. D. Wilson, B. C. Bender, D. R. McCurdy, J. E. Hall, R. R. Tidwell, A. Kumar, M. Bajic and D. W. Boykin, *J. Med. Chem.*, 1998, **41**, 3872–3878.
8 D. Zhang and M.-J. Dumont, *J. Polym. Sci., Part A:Polym. Chem.*, 2017, **55**, 1478–1492.
9 A. F. Sousa, C. Vilela, A. C. Fonseca, M. Matos, C. S. R. Freire, G.-J. M. Gruter, J. F. J. Coelhob and A. J. D. Silvestrea, *Polym. Chem.*, 2015, **6**, 5961–5983.
10 D. Liu, Y. Li, C. Wang, H. Yang, R. Wang, S. Li and X. Yang, *Appl. Catal., A*, 2024, **669**, 119497–119506.
11 Y. Tao, S. Fan, X. Li, J. Yang, J. Wang and G. Chen, *J. Colloid Interface Sci.*, 2024, **654**, 731–739.
12 S. Xu, P. Zhou, Z. Zhang, C. Yang, B. Zhang, K. Deng, S. Bottle and H. Zhu, *J. Am. Chem. Soc.*, 2017, **139**, 14775–14782.
13 M. E. Fergani, N. Candu, P. Granger, S. M. Coman and V. I. Parvulescu, *Catal. Today*, 2022, **405**, 267–276.
14 Y. Qin, Y. Li, M. Zong, H. Wu and N. Li, *Green Chem.*, 2015, **17**, 3718–3723.
15 J. T. Cunha, A. Romaní and L. Domingues, *Catalysts*, 2022, **12**, 202–216.
16 S. Shi, X. Zhang, M. Zong, C. Wang and N. Li, *Mol. Catal.*, 2019, **469**, 68–74.
17 X. Pan, S. Wu, D. Yao, L. Liu, L. Zhang, Z. Yao, Y. Pan, S. Chang and B. Li, *React. Chem. Eng.*, 2020, **8**, 1397–1404.
18 A. Araya, N. Guajardo and M. E. Lienqueo, *Biochem. Eng. J.*, 2024, **202**, 109157–109162.
19 W. P. Dijkman, D. E. Groothuis and M. W. Fraaije, *Angew. Chem.*, 2014, **126**, 6633–6636.
20 J. Carro, P. Ferreira, L. Rodríguez, A. Prieto, A. Serrano, B. Balcells, A. Ardá, J. Jiménez-Barbero, A. Gutiérrez, R. Ullrich and M. Hofrichter, *FEBS J.*, 2015, **282**, 3218–3229.
21 H. Jia, M. Zong, H. Yu and N. Li, *ChemSusChem*, 2017, **10**, 3524–3528.
22 A. Swoboda, S. Zwölfer, Z. Duhović, M. Bürgler, K. Ebner, A. Glieder and W. Kroutil, *ChemSusChem*, 2024, **17**, e202400156.
23 H. Jia, M. Zong, G. Zheng and N. Li, *ChemSusChem*, 2019, **12**, 4764–4768.
24 A. Karich, S. B. Kleeberg, R. Ullrich and M. Hofrichter, *Microorganisms*, 2018, **6**, 1–12.
25 D. S. Choi, Y. Ni, E. Fernández-Fueyo, M. Lee, F. Hollmann and C. B. Park, *ACS Catal.*, 2017, **7**, 1563–1567.
26 W. Zhang, B. O. Burek, E. Fernández-Fueyo, M. Alcalde, J. Z. Bloh and F. Hollmann, *Angew. Chem., Int. Ed.*, 2017, **56**, 15451–15455.
27 J. H. Jang, J. E. Park and J. S. Han, *Eur. J. Pharmacol.*, 2018, **284**, 152–156.
28 X. Zhang, Z. Tan, C. Li, S. Qi, M. Xu, M. Li, W. Xiong, W. Zhuang, D. Liu, C. Zhu and H. Ying, *Bioresour. Bioprocess.*, 2021, **8**, 1–9.

29 Z. Tan, X. Zhang, M. Xu, Y. Fu, W. Zhuang, M. Li, X. Wu, H. Ying, P. Ouyang and C. Zhu, *Sci. Adv.*, 2022, **8**, 1912–1921.
30 X. Zhang, Z. Tan, M. Xu, W. Zhuang, H. Ying, Z. Chu and C. Zhu, *Green Synth. Catal.*, 2023, **5**, 153–158.
31 S. M. McKenna, P. Mines, P. Law, K. Kovacs-Schreiner, W. R. Birmingham, N. J. Turner, S. Leimkühlerd and A. J. Carnell, *Green Chem.*, 2017, **19**, 4660–4665.
32 Z. Wu, L. Shi, X. Yu, S. Zhang and G. Chen, *Molecules*, 2019, **24**, 3648–3664.
33 D. del-Bosque, J. Vila-Crespo, V. Ruipérez, E. Fernández-Fernández and J. M. Rodríguez-Nogales, *Gels*, 2023, **9**, 320–336.
34 W. Cheng, J. Zhang, J. Liu and Z. Yu, *VIEW*, 2020, **1**, 20200060–20200067.